JOURNAL OF AIRCRAFT
Vol. 36, No. 5, September–October 1999

Simple Description of Airflow Characteristics Inside an Unfolding Parachute

Jean Potvin*
St. Louis University, St. Louis, Missouri 63156-0907

A simple calculation of the airflow velocity and pressure inside a round parachute unfolding during the inflation stage that precedes full parachute expansion is described. On the basis of photographic sequences of deployments in the field, the parachute is assumed to adopt the shape of a tubular sock as it unfolds from an elongated collapsed or folded state. The effects of the unfolding process are described by the motion of the transition region between folded and unfolded fabric (called the unfolding front), a region that moves like a traveling pulse up the parachute's longitudinal axis. Such a motion is determined by the energy-dissipating nature of fabric unfolding and is coupled to the motion of the air column entering the sock. An interesting prediction is that the translation velocity of the unfolding front rapidly reaches a constant value, or terminal velocity, which may be significantly lower than the air speed of the wind entering the parachute. A comparison with experimental data collected by the U.S. Army and the U.S. Air Force confirms this feature. The paper ends with a discussion on using the model to generate improved sets of initial conditions for the structure-coupled computational fluid dynamics codes that are used to simulate parachute inflation.

Nomenclature

A = cross-sectional surface area of parachute initial shape (tubular sock)
C_D = drag coefficient of fully or partly unfolded sock under steady-state flow conditions
C_T = drag coefficient of tubular sock during unfolding
D_0 = constructed diameter of parachute
F_{inertial} = reaction force generated by inertia of fabric in contact with air cap
F_{ramair} = ram force pushing air into tubular sock
F_{unfold} = aerodynamic unfolding force applied on end cap
$G(t)$ = pressure time profile function
L = unfolding characteristic length
l = fully unfolded length of tubular sock; less than a chute's radius $D_0/2$
P = pressure distribution inside inflated portion of parachute
P_∞ = upstream and downstream pressure at infinity
q = dynamic pressure associated with u_∞
t = time
t_f = time for tubular sock to completely unfold
U = terminal velocity of unfolding front
u = axial component of air velocity profile inside inflated portion of parachute
u_∞ = upstream and downstream air speed at infinity
x = axial coordinate inside unfolded portion of parachute
$x_c(t)$ = location of air end cap pressing against unfolding front
Z_0 = velocity ratio defined in Eq. (11)
$\Delta P(t)$ = pressure difference between air-cap location and $x = 0$, at arbitrary time t
ΔP_0 = assumed time-independent pressure difference between air-cap location and $x = 0$
$\Delta P_{0,\infty}$ = difference between upstream pressure at infinity and internal pressure at $x = 0$
δ = thickness of the air cap
μ = air viscosity
ρ = air density
σ_{fabric} = mass density of unfolding fabric (mass per unit surface)

Received 31 December 1997; revision received 23 December 1998; accepted for publication 21 February 1999.

*Associate Professor, P.O. Box 56907, Department of Physics, Parks College of Engineering and Aviation. Member AIAA.

Introduction

THE accurate first-principle simulation of the structural and fluid dynamics that develop during the unfolding and inflation of a parachute represents one of the great challenges faced today by the computational sciences.[1,2] Unlike the computer simulations of fluid flow near rigid structures such as buildings or vehicles, flow simulations for inflating or gliding parachutes involve real-time feedback between the position of a large number of structural parts, i.e., parachute fabric and suspension-line elements, and the air flow near those same structural parts. Moreover, the parachutes' lack of rigidity is the source of very complex and unsteady types of fluid flow, particularly during inflation.

The results from a first series of structure-coupled computational fluid dynamics (CFD) simulations of parachute dynamics have been published and discussed recently.[2–9] Representing a first-generation attempt at solving this problem, these simulations have focused on the general characteristics of the flow inside an inflating or inflated parachute, leaving out or approximating the effects of several factors that cannot be simulated efficiently with current algorithms or computing power. For example, the effects of wrinkled fabric and other structural elements not under tension are left out. Likewise, structural elements getting into contact are allowed to pass through each other. These factors do not seriously compromise the accuracy of these recent simulations because the flight regimes under consideration involved well-separated structures that are under tension, such as during the late stage of parachute inflation or the glide phase of inflated parachutes. However, these structure-coupled CFD codes need to be developed further to become accurate tools for the investigation of other aspects of parachute inflation, such as fabric unfolding or inflation of limp fabric.

Fabric unfolding is an important aspect of inflation because it determines the initial conditions from which the airflow inside and outside of a spreading canopy will evolve (Fig. 1). In fact, unfolding and early inflation are important stages at which a significant portion of the energy carried by the air rushing inside the parachute is transferred out to the unfolding fabric as well as to the airflow outside and behind the parachute. Thus, unfolding and early inflation could lead to noticeable differences between the internal and external flow velocities and pressure. As discussed in this paper,

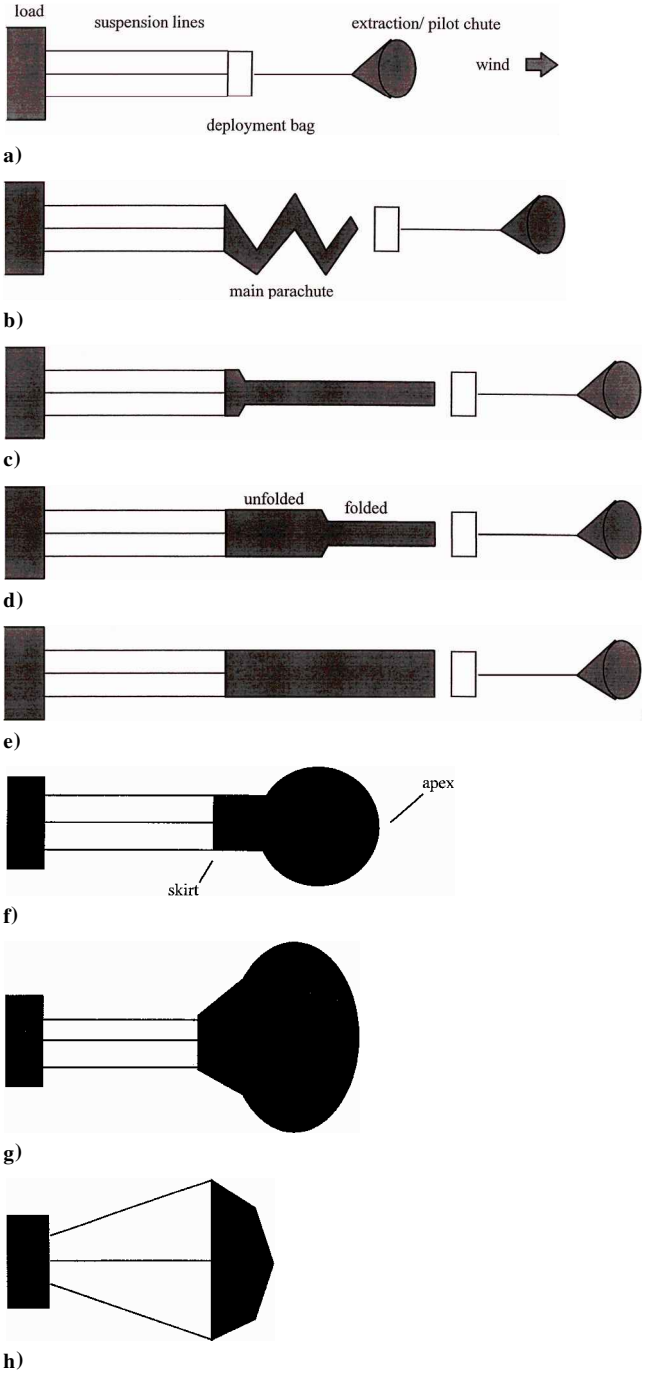

Fig. 1 Schematics of unfolding and inflation processes taking place during the deployment of a circular parachute.[10] Steps a and b: bag and main parachute deployment. Steps c–e: main parachute unfolding and early inflation. Steps f–h: late inflation and canopy spreading. The model discussed in this paper describes steps c, d, and e.

experimental data in fact suggest that unfolding may transfer out as much as 60% of the energy carried by the internal flow.

Certainly, such large energy transfers must be included in one form or another in CFD simulations, especially in those that begin after unfolding. Current strategies for the generation of initial conditions include using a uniform velocity field outside and inside an already-unfolded tube-shaped parachute, or the simulation of air being blown into an unfolded, fixed-shape tubular parachute. However, because such generated initial flow explicitly ignores fabric unfolding, it is not clear whether the calculated initial velocities and pressures at early times are realistic.

The aim of this paper is to introduce a simple analytical model that supplies more realistic initial conditions to postunfolding CFD simulations. The model is defined by events C through E in Fig. 1 and takes advantage of the inherent cylindrical symmetry of the unfolding tubular sock that initially makes up the parachute. This geometry is seen clearly in numerous photographs of inflating round chutes, such as in the reefing study by Lee[10] or the inflation study by Berndt and Deweese.[11] Thus the model consists of simulating the internal airflow with a one-dimensional version of the mass conservation and Euler equations, which are solved using a time-dependent boundary at the end of the sock that takes into account the effects of fabric unfolding. The resulting equations are simple enough to be completely integrable and will yield useful information about the internal flow's spatial and temporal profiles of the velocity and pressure during the unfolding sequence.

Simple Model of Unfolding and Early Inflation

Hypotheses and Approximations

Based on photographs and video footage of actual inflation sequences of round parachutes,[10,11] Fig. 1 shows schematics of the unfolding and early inflation of a sock that makes up the parachute during this stage of deployment. The sock is shown inflating into a tube from a longitudinal collapsed or folded state. The sock is stretched longitudinally as a result of the suspension lines and extraction pilot chute pulling the parachute skirt and apex in opposite directions. Note that the fabric in this initially collapsed state may still be folded, as sketched in Fig. 2. Most of the fabric motion follows the area of transition between the folded and unfolded portions of the parachute, here called the unfolding front, which moves like a traveling pulse along the parachute's longitudinal axis. Video footage shows that most unfolding parachutes display some small changes of the tube's radius until the unfolding front reaches the apex of the parachute. During unfolding, the fabric appears to bear little loading, a function that is carried out mostly by the radial tapes linking the parachute gores together.

The model assumes that none of the energy carried by the air rushing into the sock is spent in changing its thermodynamical state and density but is used rather in changing the motion of the fabric and airflow inside and outside of the sock. This contrasts with car air bag inflation dynamics in which gas expansion involves significant changes of the gas temperature and density, thus requiring the use of thermodynamics.[12,13]

It also is assumed that the parachute's drag is not high enough to decelerate the system substantially during this early stage of inflation. Given the very short timescales involved, this assumption means that the airflow speed at the mouth of the parachute remains essentially constant.

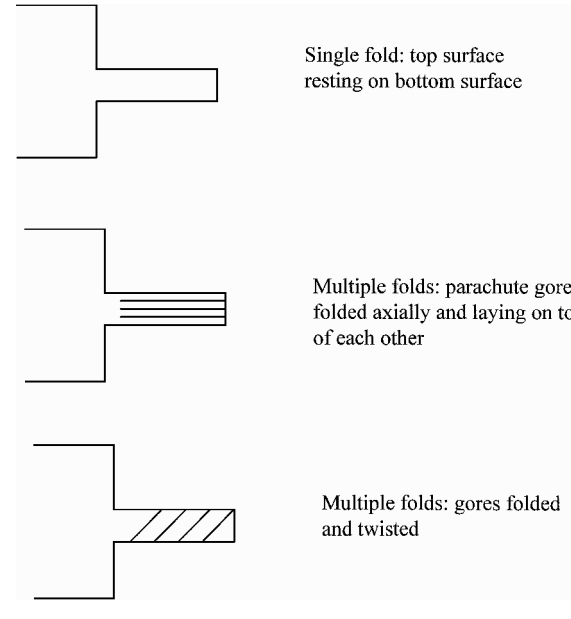

Fig. 2 Parachute folding types.

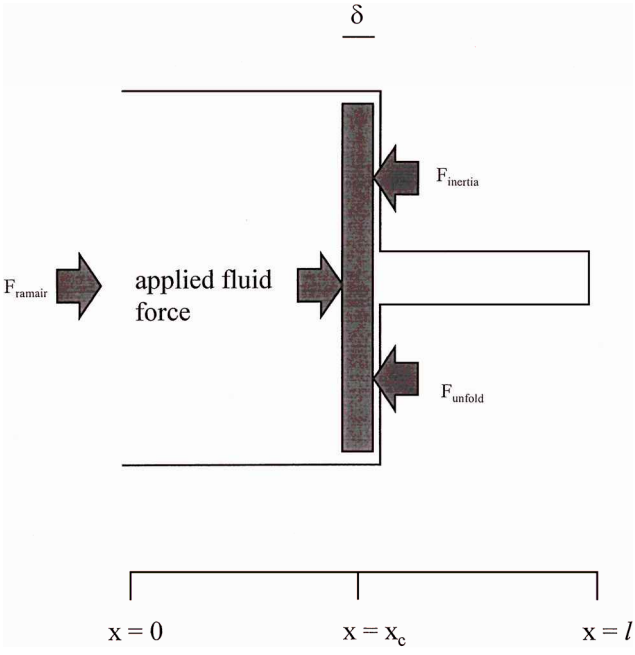

Fig. 3 Balance of forces acting on the air end cap that interacts with the fabric unfolding front.

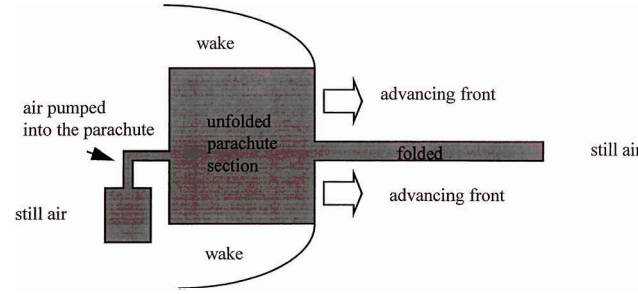

a) Sealed parachute or air bag inflated by a tank of compressed air

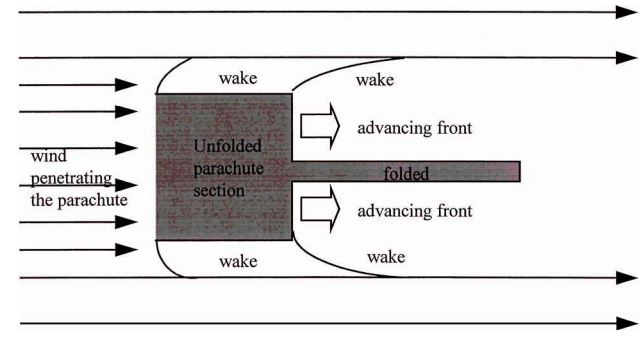

b) Open-end parachute inflated by environmental airstream

Fig. 4 Wake creation by an advancing unfolding front.

A detailed experimental study of canopy inflation by Berndt and Deweese[11] shows that there is some radial expansion of the inflated portion of the tubular sock during the unfolding process, amounting to about 10–20% of the parachute's "flat" radius. Such a small amount of radial expansion is the reason for the model, which consists of considering the sock's inflation process as being defined by a fixed-radius column of air entering the parachute. The model further describes the column as pushing an air end cap, or air cap, causing fabric to unfold. Figure 3 shows the forces involved on the end cap, which is located at x_c next to the unfolding fabric. The end cap has an average width δ and cross-sectional area A. Moreover, the effects of gravity are neglected and incompressible flow is assumed.

Given the basic one-dimensional geometry of the problem, the dynamics for the motion of the fluid inside the sock therefore is determined by the one-dimensional versions of the mass conservation equation and the Navier–Stokes equation[14,15]:

$$\frac{\partial u}{\partial x} = 0, \qquad 0 < x \leq x_c \tag{1}$$

$$\frac{\partial u}{\partial t} + u\frac{\partial u}{\partial x} = -\frac{1}{\rho}\frac{\partial P}{\partial x} + \frac{\mu}{\rho}\frac{\partial^2 u}{\partial x^2}, \qquad 0 < x < x_c \tag{2}$$

This set of equations is supplemented by the equation of motion of the air cap itself, which is viewed as a body separate from the fluid entering the sock (Fig. 3). Its motion is determined by the balance of three internal and external forces, namely, the unfolding fabric-generated force F_{unfold}, the ram-air force F_{ramair}, which corresponds to the air column pushing the air cap inside the sock, and the reaction force F_{inertia} generated by the inertia of the unfolding fabric elements that are in contact with the air cap. Such forces thus give rise to the following equation of motion:

$$\rho\delta A\frac{\mathrm{d}u(x_c, t)}{\mathrm{d}t} = F_{\text{ramair}} - F_{\text{inertia}} - F_{\text{unfold}} \tag{3}$$

A specific form for the fabric unfolding force F_{unfold} is written by first assuming that there is little or no transverse fabric motion in the unfolded portions of the parachute. This means that most of the energy that transfers out of the parachute does so at the location of the unfolding front. Moreover, as suggested by Fig. 4, the advancing front encounters air resistance in a way similar to that of any solid moving through a fluid because the front's motion and unfolding action combine to create a wake. Depending on the type of airflow existing in the parachute's environment, the created wake may follow or precede the front (Fig. 4). Neglecting the energy transferred into fabric kinetic energy and fabric tension, the force F_{unfold} acting on the air end cap should be, to a large part, of a dissipative nature and thus given by the following expression:

$$F_{\text{unfold}} = \tfrac{1}{2}\rho C_T A u(x_c, t)^2 \tag{4}$$

Here C_T would include both contributions to drag of the sock's instantaneous shape and of the unfolding fabric. Its value also would depend on the type and complexity of the folds (see Fig. 2). Finally, its value would depend on the flowfield characteristics of the sock's environment (Fig. 4), in particular on the speed u_∞ of the flow entering the sock. At the moment, the value of C_T is unknown and will only be determined empirically.

On the other hand, the force F_{ramair} represents the action of the air column pushing on the end cap and is given by the pressure difference in front of the cap, $P(x_c - \delta/2, t)$, and behind the cap, $P(x_c + \delta/2, t)$. This pressure difference is rewritten using an approximate relationship that expresses the pressure behind the cap in terms of the pressure at the mouth of the sock and of the air column overall drag in a steady flow, namely,

$$P(x_c + \delta/2, t) \approx P(0, t) - \tfrac{1}{2}\rho C_D u_\infty^2 \tag{5}$$

Defining $\Delta P(x_c, t)$ as $[P(x_c - \delta/2, t) - P(0, t)]$, one obtains

$$F_{\text{ramair}} = \Delta P(x_c, t)A + \tfrac{1}{2}A\rho C_D u_\infty^2 \tag{6}$$

In principle, the value of the pressure differential ΔP is a time-dependent function. However, our lack of detailed knowledge of the process forces us to assume such a differential to be constant in time. For clarity, the constant ΔP is relabeled as ΔP_0. This approximation should be accurate enough for cases in which $\Delta P \ll 0.5\rho u_\infty^2$.

Finally, the reaction force due to the inertia of unfolding fabric is derived by assuming accelerations of fabric elements that are similar in magnitude to the acceleration of the air cap. Representing the mass of the fabric in contact with the air cap by the surface density σ_{fabric}, we obtain

$$F_{\text{inertia}} = \sigma_{\text{fabric}} A\frac{\mathrm{d}u(x_c, t)}{\mathrm{d}t} \tag{7}$$

The value of σ_{fabric} is the fourth and last parameter of the model. It is likely that C_T and C_D will depend on its value, given that basic unfolding dynamics, e.g., wakes and rates, will depend on the specific amount of inertia carried by the fabric being unfolded.

Remarks on Other Neglected Two-Dimensional Effects

As discussed earlier, using a one-dimensional description of sock unfolding and inflation applies only to cases in which there is no or little radial expansion of the inflated portion of the canopy. However, adopting a one-dimensional set of fluid equations also means that there can be no significant flow across the parachute's surface via the fabric's pores or gaps that are sometimes cut into gores to enhance stability and/or steerability.[16] Nevertheless, assuming such a "no cross-cloth flow" is a good approximation in a large number of parachute canopies because many are constructed out of low-permeability or nonpermeable cloth for increased durability.

The present formalism also grossly simplifies the fluid dynamics that occur near the parachute's mouth or "skirt," which is located at $x = 0$. The reason is that such a region is one where the incoming air is slowed as it enters the parachute, thus leading to a pressure gradient inside and outside the skirt that will decelerate the entering air as well as deflect some of it outward and outside the parachute. Clearly, the skirt region is aerodynamically more complex than the assumed airflow discussed in this paper.

Solution and Analysis

Unfolding Front Translation Speed

A one-dimensional analytical solution of Eqs. (1–7) is obtained the usual way, first by noticing that the equation of mass conservation implies that $u(x, t) = u(t)$ and then by applying the operator $\partial/\partial x$ on Eqs. (2), an operation that yields Poisson's equation $\partial^2 P/\partial x^2 = 0$ and corresponding solution,

$$P(x, t) = G(t)x + P(0, 0) \tag{8}$$

The value of function $G(t)$ is calculated from Eq. (2) once $u(t)$ is known. The latter is obtained by integrating Eq. (3) using Eqs. (4–7). Assuming $u(0) = u_\infty$ and defining the constants

$$q = \tfrac{1}{2}\rho u_\infty^2 \tag{9}$$

$$U = u_{00}\sqrt{C_D/C_T}\sqrt{1 + \Delta P_0/qC_D} \tag{10}$$

$$Z_0 = (u_\infty - U)/(u_\infty + U) \tag{11}$$

$$L = \frac{2(\rho\delta + \sigma_{\text{fabric}})}{\rho C_T} \tag{12}$$

one obtains

$$u(t) = U\frac{\left(1 + Z_0 e^{-2tU/L}\right)}{\left(1 - Z_0 e^{-2tU/L}\right)} \tag{13}$$

Here $0 < Z_0 < 1$ because $u_{00} > U$. Equation (13) is typical of systems that reach a terminal velocity because of a velocity-dependent force. As shown in Fig. 5, constant U assumes the role of a terminal speed, which here arises as a manifestation of the balance between the external force that drives the air into the sock and the fabric forces developing during the unfolding process. In practice, the airflow should be close to a steady state after a time interval set by the ratio L/U. Being proportional to σ_{fabric} and $(C_T)^{-1/2}$, such a time interval increases with the fabric mass density but decreases with the force coefficient associated with unfolding. Note also that the ratio L/U is explicitly independent of the size of the parachute, although a weak dependence on this parameter could develop through C_D. Finally, constant L appears to define a natural length scale for this problem, which in this case is set by the ratio $\sigma_{\text{fabric}}/\rho C_T$ assuming $\rho\delta \ll \sigma_{\text{fabric}}$.

A final remark: The solution derived in this section was obtained assuming a flow velocity $u(t)$ greater than the terminal velocity U, a scenario that describes most realistic parachute systems. However, parachutes deployed at low speed may be described by solutions of Eq. (3) that are characterized by the conditions $u(t) < U$ and $u(0) = 0$. The form of the solution in such a case resembles Eq. (13), with the difference that $u(t)$ is instead a function that increases with time, approaching a constant value equal to U after a time interval much greater than L/U.

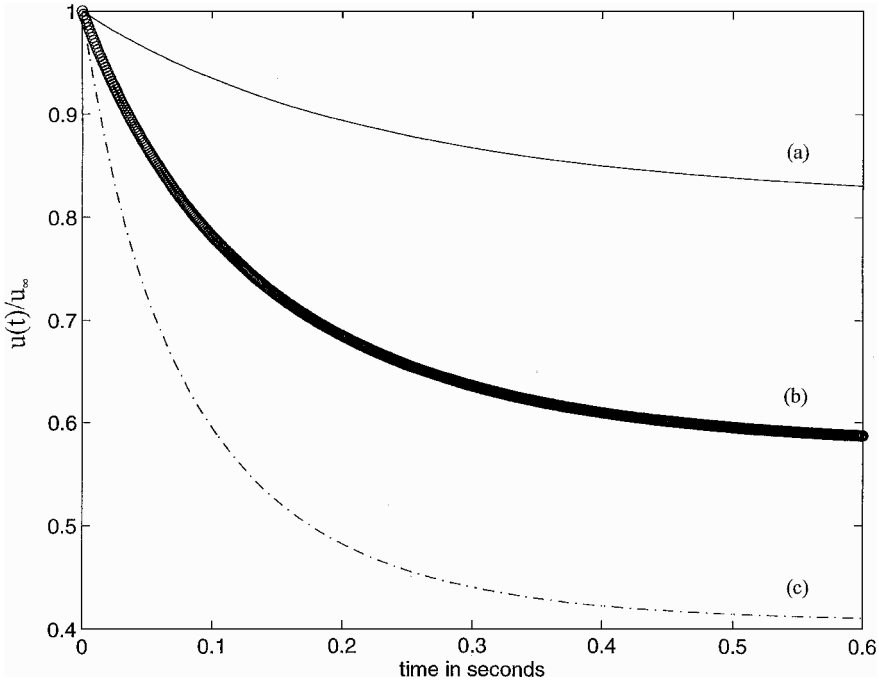

Fig. 5 Time dependence of air column and air-cap velocity: (u_∞ = 50 ft/s, C_D = 1.0, and $\Delta P_0/q$ = 0): a) C_T = 1.5 and L = 20 ft; b) C_T = 3.0 and L = 10 ft; and c) C_T = 6.0 and L = 5 ft.

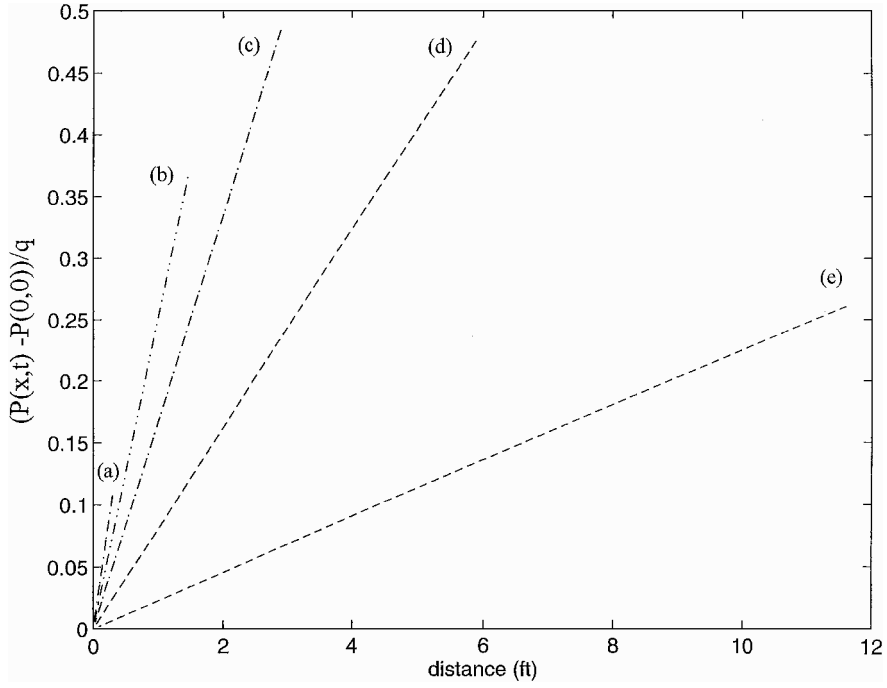

Fig. 6 Pressure excess profile $[P(x,t) - P(0,0)]/q$ along the parachute's longitudinal axis (u_∞ = 50 ft/s, C_D = 1.0, C_T = 3.0, L =10 ft, and $\Delta P_0/q = 0$): a) t = 0.01 s; b) t = 0.05 s; c) t = 0.10 s; d) t = 0.20 s; and e) t = 0.40 s. Here distance = $(U^2/u_\infty^2)X_c$.

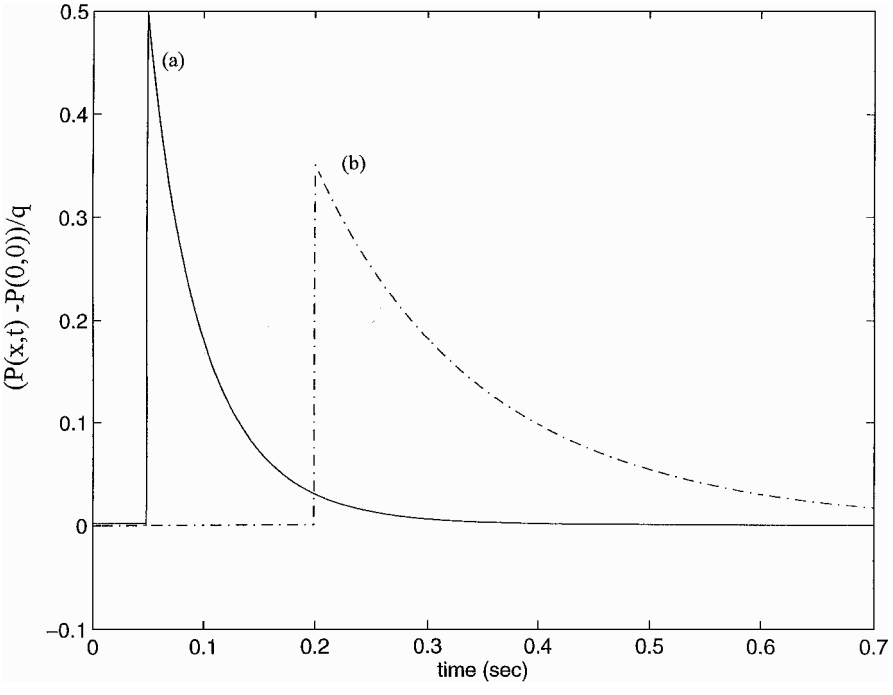

Fig. 7 Time evolution of pressure excess $[P(x,t) - P(0,0)]/q$ at a distance of 4.34(U^2/u_∞^2) ft inside the parachute (C_D = 1.0, C_T = 3.0, L = 10 ft, and $\Delta P_0/q = 0$): a) u_∞ = 150 ft/s, and b) u_∞ = 50 ft/s.

Pressure Profile Solution

Using Eq. (8) and (13) in Eq. (2) allows a direct calculation of the pressure profile and evolution inside the inflating sock, resulting in the following formula:

$$P(x,t) = 2\rho^2 U^2 C_T Z_0 \frac{x}{\rho\delta + \sigma_{\text{fabric}}} \frac{e^{-2tU/L}}{\left(1 - Z_0 e^{-2tU/L}\right)^2} + P(0,0) \tag{14}$$

Shown in Fig. 6, such a profile is characterized by pressure increasing with x. Such a picture can be understood by the fact that the combined fabric and end-cap inertia causes the airflow to decelerate, leading to a pressure buildup in front of the cap. On the other hand, the figure shows the slope $\partial P/\partial x$ to decrease with time, to a near-zero value as time becomes much greater than L/U.

The time evolution of the pressure excess $[P(x,t) - P(0,0)]$ at a given fixed point inside the parachute is shown in Fig. 7. One notices the sharp pressure increase caused by the (assumed) zero pressure difference characterizing this location when inside the folded portion of the parachute. The slower pressure decrease that follows is what is described by Eq. (14). Figure 7 also shows the unfolding spike to increase in height and to occur sooner with greater inflow speed $u(t)$.

Internal pressure also can be compared with upstream static pressure at infinity P_∞ and dynamic pressure $q = \frac{1}{2}\rho u_\infty^2$. Defined by $\Delta P_{0,\infty} \equiv P(0,t) - P_\infty = [P(0,t) - P(0,0)] + [P(0,0) - P_\infty]$, such a difference can be computed at large times when $u(t)$ is no longer time dependent, i.e., $t \gg L/U$. Using Eq. (13) and Bernoulli's principle along a streamline running from infinity to the skirt's center in a direction parallel to the parachute's longitudinal axis, one has this result $[P(0,t) - P_\infty] = q_\infty(1 - U^2/u_\infty^2)$, which yields the following formula:

$$\left.\frac{\Delta P_{0,\infty}}{q}\right|_{t=\infty} = \left[1 - \left(\frac{C_D}{C_T}\right)\left(1 + \frac{\Delta P_0}{qC_D}\right)\right] \tag{15}$$

Air-Cap Location

Because the position of the end cap x_c is defined as $\mathrm{d}x_c/\mathrm{d}t = u(t)$, the latter can be obtained by integrating Eq. (13):

$$\frac{x_c(t)}{U} = t + \frac{L}{U}\,\ell n\frac{1 - Z_0 e^{-2tU/L}}{1 - Z_0} \tag{16}$$

This result can be used to calculate the time t_f required for the sock to unfold to its length l, which is less than the chute's flat radius $D_0/2$:

$$t_f = -\frac{L}{U}\,\ell n\frac{(Z_0 - 1)e^{l/L} + \sqrt{(Z_0 - 1)^2 e^{2l/L} + 4Z_0}}{2Z_0} \tag{17}$$

For a sock made of very light fabric, i.e., small σ_{fabric}, the value of L should be small relative to l. This implies a small value of the timescale L/U, which in turn suggests that the end cap reaches its terminal velocity U early in the unfolding process. In such a case, the sock would be completely unfolded in a time interval approximated by $t_f \approx l/U < D_0/2U$. Interestingly enough, this result suggests that the sock's unfolding has a timescale like l/u_∞ just as one would naively expect, provided that the ratio C_T/C_D does not depends on u_∞.

Comparison with Experiment

The model prediction of the unfolding-front terminal speed can be checked against the data of several studies of round-parachute deployment and inflation performed by the U.S. Air Force and the U.S. Army. Furthermore, comparing data and model solutions also can give us order-of-magnitudeestimates of some of the parameters used here, in particular that of the ratio C_T/C_D.

The Air Force study was published by Berndt and Deweese[11] and involved electronic and photographic measurements of several inflation parameters characterizing over 60 deployment tests of full-scale C-9 parachutes ($D_0 = 28$ ft) and T-10 parachutes ($D_0 = 35$ ft), in the 100- to 300-ft/s speed range and 6000- to 21,000-ft altitude range. On the other hand, the Army study was carried out over several different programs at the U.S. Army Yuma Proving Ground (Harm, M., Gorman, J., Lee, C. K., Mawn, A., McIntosh, K., Watkins, J., Wallace, P., and Wellman, S., private communications, U.S. Army Soldier Systems Center—Airdrop Technology), and involved low-altitude tests on C-9s, T-10s, G-12s ($D_0 = 64$ ft), and other parachutes. The video portion of these Army data was analyzed by this author for this study and is summarized in Table 1 and in Figs. 8 and 9. Specifics of the error analysis are discussed in the Appendix.

Time Dependence of Unfolding-Front Location

Equation (16) can be compared to the results of the detailed measurements performed by Berndt and Deweese.[11] By carefully analyzing the filmed inflation sequences, they have found that the position of the apex region of the canopy can be formulated empirically as follows:

$$x_c(t) = \frac{1.275tu_\infty}{X_{\text{C-9}}}, \qquad x_c(t) = \frac{1.572tu_\infty}{X_{\text{T-10}}} \tag{18}$$

Table 1 Unfolding solid round parachute data collected during test drops performed at the U.S. Army Yuma Proving Ground[a] ($R = D_0/2$)

Parachute type, number of drops, and unfolding in clear air or in aircraft wake	R, ft	u_0, ft/s	t_f, s	$t_f u_0/R$
T-10 (3-cluster), 1 drop, clear air	17.5	421	0.16 (1)	3.86 (24)
T-10 (3-cluster), 1 drop, clear air	17.5	230	0.17 (4)	2.23 (65)
24-ft reserve (single), 11 drops, clear air	12.0	193	0.136 (7)	2.18 (11)
55-ft cargo (5-cluster), 1 drop, clear air	27.5	161	0.49 (2)	2.78 (11)
T-10 (4-cluster), 4 drops, clear air	17.5	69	0.39 (2)	1.49 (7)
T-10 (single), 1 drop, aircraft wake	17.5	166	0.10 (na)	0.92 (na)
G-12 (3-cluster), 1 drop, aircraft wake	32.0	113	0.20 (2)	0.71 (7)
G-12 (3-cluster), 1 drop, aircraft wake	32.0	98	0.20 (1)	0.61 (3)

[a]Harm et al., private communication. Numbers in parentheses indicate the errors on the last digit(s).

where the coefficients $X_{\text{C-9}}$ and $X_{\text{T-10}}$ are surface-loadingdependent with an approximate value of 6.00 ($\pm$0.30) for manned applications (note that these authors did not quote error bars on the coefficients shown in Eq. (18), although a large amount of data was used for their derivation). Such a linear time behavior is very similar to that of Eq. (16) in the limit of large time, high fabric density (compared to $\rho\delta$), and small $\Delta P_0/q$, namely,

$$x_c(t) = u_\infty\sqrt{\frac{C_D}{C_T}}t + \frac{2\sigma_{\text{fabric}}}{\rho C_T}\,\ell n\left(\frac{1}{1 - Z_0}\right) \tag{19}$$

Only in cases in which u_∞ is large are the two results identical in form, which then would suggest possible relative values for C_D and C_T , namely $C_T/C_D \sim 22$ (C-9) and 15 (T-10).

On the other hand, looking at the U.S. Army data also gives support to the model's main prediction as shown in Figs. 8 and 9. Each data point shown in the figures was obtained from video by measuring on the television screen the distance of the unfolding front relative to the canopy's skirt. As explained in more detail in the Appendix, the data are subject to errors related to the (ground-based) camera line of sight as well as low film resolution that sometimes made the identification of the unfolding front difficult. Figures 8a and 8b show the time dependence of $2x_c(t)/D_0$ for several free-falling dummy drops involving the inflation of a 24-ft-diam U.S. Army paratrooper reserve parachute, which begins unfolding at an estimated 193 ft/s (this is the third entry in Table 1). Figure 8a shows the data from a subset of four drops, along with a straight-line fit corresponding to each drop. Figure 8b shows the data from all 11 drops, without distinguishing the data from different drops; the figure also includes the straight line that best fits all data. Figure 9 shows the same observables corresponding to four unfolding/inflation sequences of one of four parachutes in a cluster of T-10 parachutes, inflating at a measured $u_\infty = 69$ ft/s. The data scatter shown in the figures is also due to random variations in airflow characteristics and parachute skirt cross-sectional area caused by the turbulent nature of the flow near the skirt; such variations are large enough to generate time-dependent distortions of the shape and size of the tubular sock. Moreover, turbulence also can start partial inflation before the complete stretching of the suspension lines.

Because of the large scatter, the results shown in Figs. 8 and 9 are obviously consistent with $x_c(t)$ being proportional to time and, consequently, would agree with most of the time dependence predicted by the one-dimensional model plotted in Fig. 10. Note that the fitted straight lines corresponding to each drop in Figs. 8 and 9 have similar slopes, which for the 24-ft- and 35-ft-diam parachutes average to 6.38 (37) s^{-1} and 2.45 (20) s^{-1}, respectively. Note also that a straight-line fitting at large times would not extrapolate back to the origin in the zero-time limit. This is, of course,

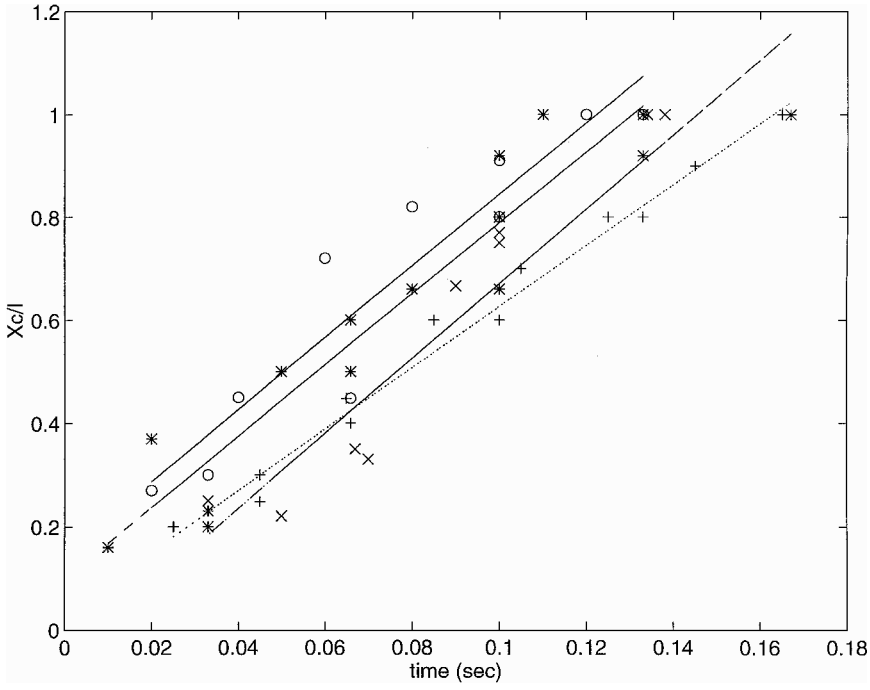

Fig. 8a Location of unfolding front vs time, as determined experimentally during test drops of a 24-ft-diam paratrooper reserve parachute at the U.S. Army Yuma Proving Ground (Harm et al., private communication). The error bar on each symbol is estimated at $\Delta\,[X_c(t)/l] \sim 0.05$–$0.10$ and, for clarity, is not shown. Each set of symbols corresponds to a different drop: drop 032 (∗), drop 033 (o), drop 034 (+) and drop 037 (×). Each straight line corresponds to a fit to the data points of a given drop.

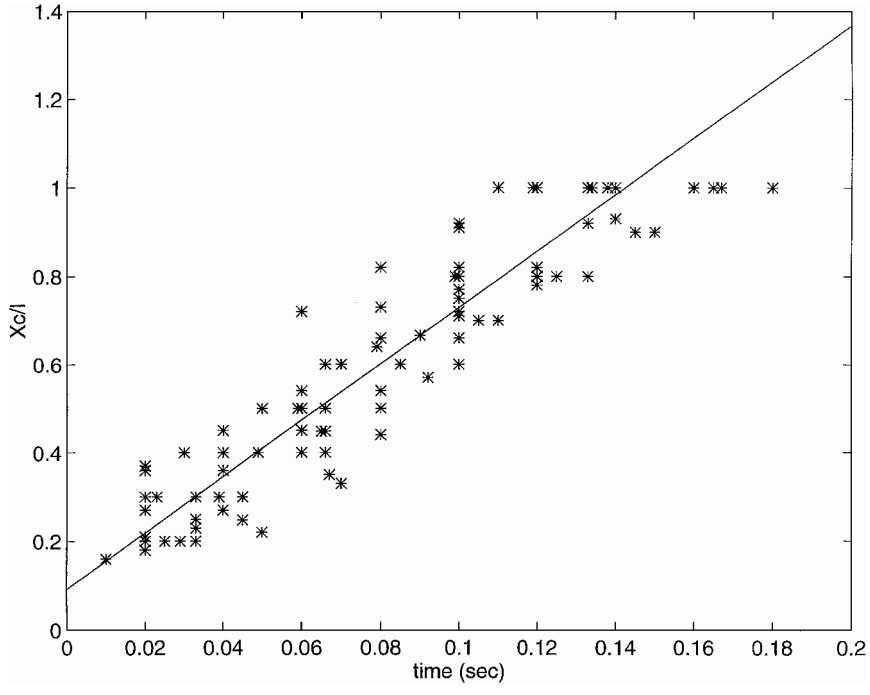

Fig. 8b Location of the unfolding front vs time, as determined experimentally during test drops of a 24 ft-diam paratrooper reserve parachute at the U.S. Army Yuma Proving Ground (Harm et at., private communication). The error bar on each symbol is estimated at $\Delta\,[X_c(t)/l] \sim 0.05$–$0.10$ and, for clarity, is not shown. The points shown include the data of Fig. 8a, as well as the data of seven other drops. The straight line corresponds to a fit of all data points.

consistent with Eqs. (16) and (19). Assuming that durations exceeding 0.02 s are "large," the straight-line fits displayed in Figs. 8b and 9 give $2x_c^{\text{fit}}(0)/D_0 = 0.091 \mp 0.030$ (24-ft-diam parachute) and $2x_c^{\text{fit}}(0)/D_0 = 0.00 \mp 0.40$ (35-ft-diam parachute; this is an average value of the four fits). These very small values are consistent with the Air Force results, i.e., Eq. (18), and suggest that the ratio $\sigma_{\text{fabric}}/\rho C_T$ in Eq. (19) should be small. Indeed, given the surface density of standard parachute fabric, which yields $\sigma_{\text{fabric}}/\rho \sim 1$ ft, and given that $\ell n[1/(1 - Z_0)] \sim 0.3$–$1.0$ (more on this below), then again, experiment implies a large value of C_T, which would be of the order of 10.

Estimates of the Terminal Velocity U

Estimates of the translation speed of the unfolding front can be obtained from the slope of the front's location time evolution curve. For manned applications, the data from the Air Force study embodied in Eq. (18) give $U/u_\infty \sim 0.21$ and 0.26 for the C-9 and T-10, respectively. In the case of the Army data, given the fact

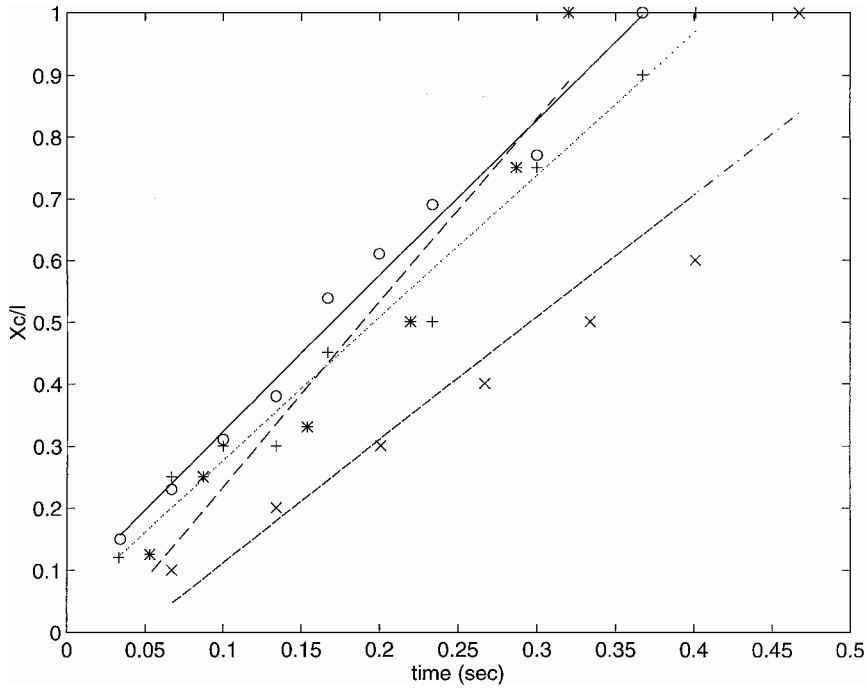

Fig. 9 Location of the unfolding front vs time, as determined experimentally during test drops of a 35-ft-diam T-10 military parachute (part of a four-cluster parachute system) at the U.S. Army Yuma Proving Ground (Harm et al., private communication). The error bar on each symbol is estimated at $\Delta\,[X_c(t)/l] \sim$ 0.05–0.10 and, for clarity, is not shown. Each set of symbols corresponds to a different drop: drop 5-136 (∗), drop 5-133 (×), drop 5-132 (+), and drop 5-130 (○). Each straight line corresponds to a fit to the data points of a given drop.

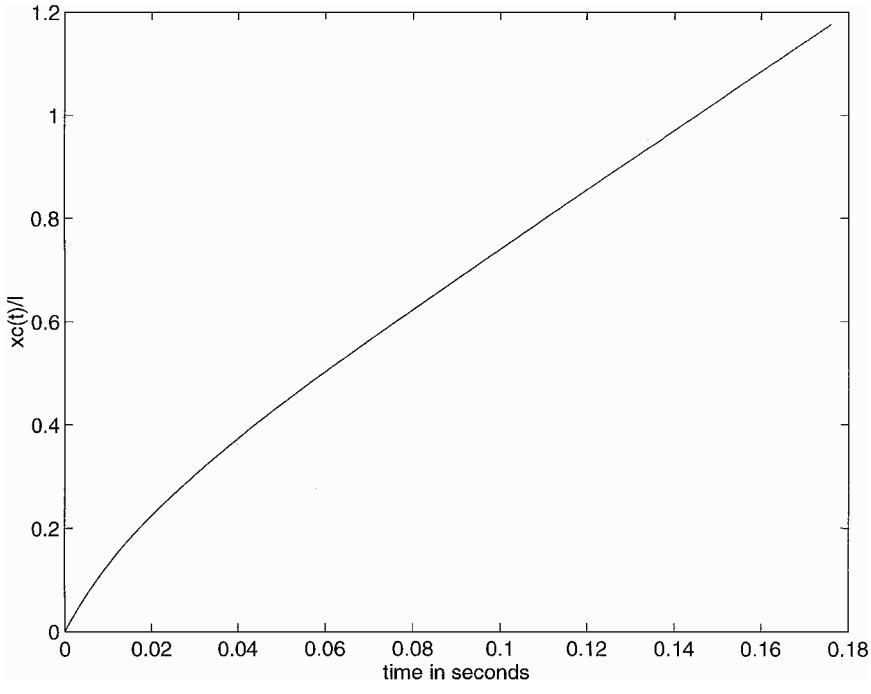

Fig. 10 Location of the unfolding front vs time. Here, C_D = 1.0, C_T = 7.6, L = 3.15 ft (to be compared with $D_0/2$ = 12 ft), and u_∞ = 190 ft/s.

that $l \sim 0.95\ (\mp 0.05)\ D_0$, we obtain $U \sim 77$–85 ft/s and $U \sim 43$–47 ft/s for the 24-ft- and 35-ft-diam parachutes, respectively. Comparing with their respective downstream airspeed, one obtains the ratio $U/u_\infty \sim 0.39 \mp 0.02$ for the 24-ft-diam parachute and $U/u_\infty = 0.62 \mp 0.04$ for the 35-ft-diam parachute. Such values show that the flow entering an unfolding parachute is decelerated by a substantial amount, leading to values of Z_0 varying between 0.25 and 0.66.

Duration of Unfolding

Table 1 shows the values for unfolding duration measured on several parachutes. Such values can be compared with the large l/L limit of Eq. (17) which results in

$$t_f \frac{2u_\infty}{D_0} = \frac{l}{U}\frac{2u_\infty}{D_0} + \frac{2u_\infty}{D_0}\frac{L}{U}\,\ell_n\left(\frac{2U}{u_\infty + U}\right)$$

$$\approx \frac{u_\infty}{U}\frac{2l}{D_0} \approx 0.95\sqrt{\frac{C_T}{C_D}} \tag{20}$$

Here, the last two steps follow from $2L/D_0 \sim 0$ and $\Delta P_0 \ll 0.5\rho u_\infty^2$. The factor 0.95 on the right-hand side was obtained from the measurements of l, which suggest $2l/D_0 \sim 0.95$ as discussed previously. Comparing Eq. (20) with the clear-air results of Table 1 would mean that $C_T/C_D \sim 2.5$–16 depending on the parachute system; using the aircraft-wake results in the simplified version of Eq. (20) would give

$C_T/C_D \sim 0.41$–0.94, thus stressing the importance of the aerodynamic environment in which a parachute is deployed.

On the other hand, using the empirical scaling formulas derived by Berndt and Deweese[11] gives

$$\frac{2t_f u_\infty}{D_0} = 0.6X_{\text{C-9}} \approx 3.9, \qquad \frac{2t_f u_\infty}{D_0} = 0.5X_{\text{T-10}} \approx 3.0 \quad (21)$$

resulting in $C_T/C_D \sim 16$ and 10 for the C-9 and T-10 parachutes, respectively. These numbers are very similar to those derived from Eq. (18) and are consistent with the clear-air numbers derived from the Army test drops. Moreover, Eqs. (18) and (21) imply that $2l/D_0 \; x_{0.8}$ for the parachutes discussed in Ref. 11.

Initial Conditions for CFD Simulations

The solutions derived from this simple model can be used to motivate a new set of procedures for generating initial conditions for structure-coupled CFD simulations of the later stages of parachute inflation (steps F–H in Fig. 1).

Figure 11 shows the general characteristics of the one-dimensional solution derived here at the very end of unfolding (i.e., $t = t_f$). The solution is mapped in the figure along with assumed airflow properties outside and away from the unfolded sock. It must be realized, however, that using such a map for defining the initial pressure and flow velocity may induce unphysical numerical transients because of the large gradients involved. This is especially critical for simulations of low-inertia structural elements such as parachute fabric. Thus a numerical preconditioning step preceding the actual simulation is proposed instead, whereby one carries out a CFD simulation of the flow inside and outside of a tube of increasing length, but of constant cross-sectional surface area. Here the length of the tube would be determined by the dynamics of the motion of a disk of mass M capping the tube. The motion of the disk would be subjected to a pushing force determined by the CFD-generated pressure difference across its surface; the disk also would be subjected to an unfolding force given by Eq. (4). In this exercise the values of C_D and C_T could be taken from the empirical determination of the preceding section. This numerical preconditioning would end at the moment the disk reaches an axial distance equal to l. The calculated fluid properties at that time thus would provide a full set of spatially smooth initial conditions for the detailed CFD simulation of an inflating and fully opening parachute.

Note that such preconditioned initial conditions would not necessarily yield a solution identical to the solution obtained analytically in this paper. Such a solution, however, would implement the basic physical picture discussed here, without some of the approximations that were called in for the purpose of solving the model analytically. For example, using preconditioning to include the parachute's exterior would provide a more realistic flowfield in the skirt area as well as near the parachute apex (see Fig. 11). As a result, the force F_{ramair} that drives the motion of the disk (i.e. unfolding) would also be more realistic.

Note also that the proposed preconditioning does not involve the calculation of fabric dynamics except for the unfolding motion itself, as in the model discussed in this paper. However, structural observables such as the gore radial stitching tape tension could be estimated from the known tape elastic properties and the calculated values of the tube drag force obtained during the preconditioning. On the other hand, fabric tension itself should be small because, as seen in the video of real deployments, the fabric is generally loose. Here the gore radial tapes appear to bear most of the load during unfolding.

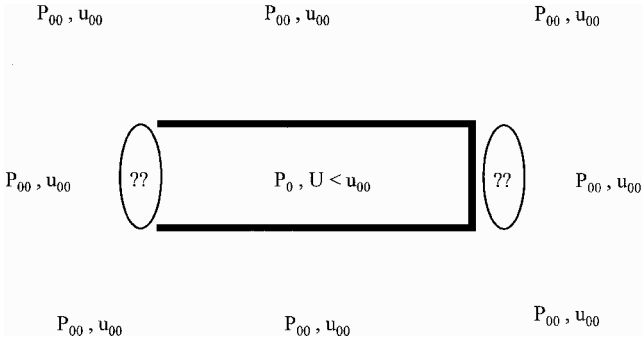

Fig. 11 Assumed external flow characteristics and calculated internal flow characteristics using the one-dimensional model.

Conclusions

The one-dimensional model presented in this paper is an attempt at understanding in simple terms the dynamics of fabric unfolding during parachute inflation. The model emphasizes the energy dissipation aspect of unfolding rather than the accumulation of fabric potential energy or changes of fabric kinetic energy. Its most interesting predicted dynamics are certainly the existence of a terminal speed reached by the unfolding front after a short deceleration, a feature common to objects under a velocity-dependent force. Data gathered by the U.S. Air Force and U.S. Army appear to confirm this trend. Moreover, the empirical determination of the model input parameters points to substantial flow speed reductions inside of the parachute during the unfolding process.

Besides its simplicity and pedagogical value, the greatest use of the model and ideas discussed here will be in their implementation as initial conditions in structure-coupled CFD simulations of inflation. The use of the model in CFD simulations also should permit interesting sensitivity investigations of structure-coupled CFD simulations on various types of initial conditions, with regard to overall parachute inflation characteristics such as maximum load and filling time.

Appendix: Sources of Systematic Errors in the Analysis of the U.S. Army Data

The video data collected at the U.S. Army Yuma Proving Ground (Harm et al., private communication) was recorded from the ground, using standard- and high-speed cameras. Each video frame bears a time stamp that marks time down to a thousandth of a second (Harm et al., private communication). Thus the time evolution of the unfolding front could be followed at a very short timescale. Such a method, however, involves two sources of errors.

Line-of-Sight Error

Although the cameras were located at a large enough horizontal distance from the point of parachute opening, the measured values of $x_c(t)$ do contain an unknown systematic error related to the unfolding sock's longitudinal axis not being perpendicular to the cameras' line of sight. In principle, such an error will affect each measurement of $x_c(t)$ differently by contributing a time-dependent factor proportional to the cosine of the angle defined by the parachute axis and the continuously changing line of sight of a given camera due to the parachute's fall. However, this angle should be considered constant, given the extreme brevity of sock unfolding, which in this case means that the cosine factor will cancel out in the ratio $x_c(t)/l$ (provided that l also is measured on the television screen).

Unfolding-Front Identification Error

A frame-by-frame analysis of the unfolding front's motion is limited by many factors that include degraded image clarity and lack of details due to the great distance separating camera and parachute. Another factor concerns parachute cluster inflation, where the front progression is masked by the other parachutes that inflate in the background. Finally, the fact that the unfolding front is not always a blunt end cap, but rather a "pointy" one, also limits the accuracy of the analysis. For these reasons, each data point shown in Figs. 8 and 9 should be associated with error bars approximating $\Delta[X_c(t)/l] \sim 0.05$–$0.10$. These error bars are not displayed in the figures for the sake of graphical clarity.

Acknowledgments

The author would like to thank S. Ahmed from Parks College, and R. Benney and K. Stein from the U.S. Army Soldier Systems Center/

Airdrop Technology, U.S. Army Natick Research, Development, and Engineering Center (NRDEC), for many fruitful discussions on the topic of CFD simulations. He also thanks M. Harm, J. Gorman, C. K. Lee, A. Mawn, K. McIntosh, J. Watkins, P. Wallace, and S. Wellman from NRDEC, and V. L. Behr from Sandia National Laboratories for providing the parachute inflation data so essential to this study. The author is grateful to C. K. Lee and NRDEC's Airdrop Technology Team (formerly Mobility Directorate) for their generous hospitality during his sabbatical leave where this manuscript was written. Finally, he wishes to thank G. Peek, Parks College Parachute Research Group, for many fruitful discussions and suggestions.

References

[1]Peterson, C. W., Higuchi, H., and Strickland, J. H., "The Fluid Dynamics of Parachute Inflation," *Annual Review of Fluid Mechanics*, Vol. 28, Annual Review, Inc., Palo Alto, CA, 1996, pp. 361–387.

[2]Higuchi, H., and Strickland, J. H., "Parachute Aerodynamics: An Assessment of Prediction Capability (1995)," *13th AIAA Aerodynamic Decelerator Systems Technology Conference*, AIAA, Washington, DC, 1995, pp. 1–16; AIAA Paper 95-1531.

[3]Benney, R. J., and Stein, K. R., "Computational Fluid-Structure Interaction Model for Parachute Inflation," *Journal of Aircraft*, Vol. 33, No. 4, 1996, pp. 730–736.

[4]Stein, K. R., Benney, R. J., Kalro, V., Johnson, A. A., and Tezduyar, T. E., "Parallel Computation of Parachute Fluid-Structure Interactions," *14th AIAA Aerodynamic Decelerator Systems Technology Conference*, AIAA, Reston, VA, 1997, pp. 277–284; AIAA Paper 97-1505.

[5]Stein, K. R., Benney, R. J., Kalro, V., Leonard, J. W., and Accorsi, M. L., "Current 3-D Structural Dynamics Finite Element Modeling Capabilities," *14th AIAA Aerodynamic Decelerator Systems Technology Conference*, AIAA, Reston, VA, 1997, pp. 285–303; AIAA Paper 97-1506.

[6]Ibos, C., Lacroix, C., Chuzet, L., and Granville, D., "SINPA, a Full 3D Fluid-Structure Software for Parachute Simulation," *14th AIAA Aerodynamic Decelerator Systems Technology Conference*, AIAA, Reston, VA, 1997, pp. 313–323; AIAA Paper 97-1508.

[7]Chuzet, L., "Numerical Determination of Parachute Performances with SINPA Software," *14th AIAA Aerodynamic Decelerator Systems Technology Conference*, AIAA, Reston, VA, 1997, pp. 324–334; AIAA Paper 97-1509.

[8]Peterson, C. W., Strickland, J. H., Wolfe, W. P., Sundberg, W. D., and McBride, D. D., "Development of a Massively Parallel Parachute Performance Prediction Code," *14th AIAA Aerodynamic Decelerator Systems Technology Conference*, AIAA, Reston, VA, 1997, pp. 268–276; AIAA Paper 97-1504.

[9]Mosseev, Y., "The Multipurpose Integrated PC-Software for Structural and Aeroelastic Analysis of Decelerators, Paragliders and Balloons," *14th AIAA Aerodynamic Decelerator Systems Technology Conference*, AIAA, Reston, VA, 1997, pp. 128–138; AIAA Paper 97-1455.

[10]Lee, C. K., "Radial Reefing Method for Accelerated and Controlled Parachute Opening," *Journal of Aircraft*, Vol. 31, No. 5, 1994, pp. 1124–1129.

[11]Berndt, R. J., and Deweese, J. H., "Filling Time Prediction Approach for Solid Cloth Type Parachute Canopies," *1st AIAA Aerodynamic Decelerator Systems Technology Conference*, AIAA, Reston, VA, 1996, pp. 17–32.

[12]Wang, J. T., and Nefske, D. J., "A New CAL3D Airbag Inflation Model," SAE-880654, Society of Automotive Engineers, 1989, pp. 4.687–4.706.

[13]Mestreau, E., and Lohner, R., "Airbag Simulation Using Fluid/Structure Coupling," AIAA-96-0798, 1996, pp. 2–8.

[14]Kuethe, A. M., and Chow, C.-Y., *Foundations of Aerodynamics*, 4th ed., Wiley, New York, 1986, pp. 449–461.

[15]Fox, R. W., and McDonald, A. T., *Introduction to Fluid Mechanics*, 4th ed., Wiley, New York, 1992, pp. 232–236.

[16]Knacke, T. W., *Parachute Recovery Systems Design Manual*, Para, Santa Barbara, CA, 1992.